Published in IET Communications
Received on 8th February 2011
Revised on 6th April 2011
doi: 10.1049/iet-com.2011.0134

ISSN 1751-8628

Graph-based interference coordination scheme in orthogonal frequency-division multiplexing access femtocell networks

K. Zheng[1] *Y. Wang*[1] *C. Lin*[2] *X. Shen*[3] *J. Wang*[4]

[1]*Wireless Signal Processing and Network Lab Key laboratory of Universal Wireless Communication, Ministry of Education Beijing University of Posts and Telecommunications, Beijing 100088 People's Republic of China*
[2]*Department of Computer Science and Technology, Tsinghua University, Beijing 100084, People's Republic of China*
[3]*Department of Electrical and Computer Engineering, University of Waterloo, Waterloo, Ontario, Canada N2L 3G1*
[4]*China Unicom Research Institute, Beijing 100032, People's Republic of China*
E-mail: zkan@bupt.edu.cn

Abstract: Femtocell technology has gained widespread attention recently due to its advantages, such as infrastructure cost reduction, improved service coverage and high data throughput in indoor environments. As femtocell networks are customer-deployed without proper network planning, their interference environment tends to be much more complicated than traditional cellular networks. The authors present the framework of channel allocation in orthogonal frequency-division multiplexing access (OFDMA) femtocell network with the graphical approaches. A novel graph-based interference coordination scheme is proposed to maximise the system throughput while ensuring proportional rate fairness among femtocells. The scheme explicitly uses the received signal-to-interference-plus-noise-ratio to generate the interference graph of OFDMA femtocell networks, so as to guarantee the acceptable inter-cell interference for all the links. First, all the femtocells are partitioned into different groups by applying a greedy graph colouring algorithm to maximise the sum throughput of each group. The femtocells in the same group share the assigned subchannels while those in different groups are allocated to orthogonal subchannels. Then, an optimisation problem is formulated to determine the number of subchannels assigned to each group. Further, an approximation method is proposed to solve the optimisation problem. Simulation results are conducted to demonstrate the effectiveness of the proposed scheme in terms of throughput and fairness index.

1 Introduction

Femtocell technology has been applied extensively to high-speed wireless communication systems, such as WCDMA, CDMA2000 and WiMAX due to its potential advantages such as improved indoor coverage, energy efficiency and low cost [1–3]. Also, it will be included into the third-generation (3G) long-term evolution (LTE) networks and its advancement (LTE-A) as one of the key features [4]. Compared with macrocells, the femtocells provide better radio link quality to the users while consuming less power of mobile devices in indoor environments. For operators, a significant amount of traffic can be moved from the macrocell network to the femtocell network, which can reduce the deployment cost. However, this technology is still under development and there are many issues needed to be addressed such as access control, timing and synchronisation, and interference coordination [5].

On the other hand, owing to its efficient utilisation of the available frequency bandwidth and robustness to frequency-selective fading environments, orthogonal frequency-division multiplexing access (OFDMA) has been accepted as a multiple access method in 3G LTE and LTE-A networks for downlink transmissions. In OFDMA-based systems, users are multiplexed in frequency by means of a scheduler, which assigns subcarriers and time slots to different users according to the pre-defined scheduling metrics. Subcarriers can be orthogonally allocated to different users at the cost of system throughput. However, dense reuse of available subcarriers is envisaged in the future networks in order to increase the transmission data rate, which may cause strong co-channel interference and limit the network throughput especially for the cell-edge users. So, developing an efficient radio resource allocation scheme for interference coordination in OFDMA networks is of significant interest to academic and industry. Based on the requirement of the inter-base station (BS) communication interval, most of the existing and currently being developed interference coordination strategies can be categorised into three types, that is, the static, semi-static and dynamic strategies. The static and semi-static strategies, which need inter-BS communication to be done on a time scale of seconds or longer, have already gained much attention in 3G LTE cellular networks due to their reasonable implementation complexity and overhead [6]. Typical strategies, such as static soft frequency reuse (SFR)

[7] and fractional frequency reuse (FFR) [8], utilise the resources of frequency and radiated power to coordinate BS transmissions with pre-defined resource constraints for different types of users. These strategies can significantly improve the performance of cell-edge users. Besides these, the dynamic strategies are also proposed to mitigate the inter-cell interference, where the information such as the user location and channel states are needed [9].

As femtocell networks are customer-deployed without proper network planning, their interference environment tends to be much more complicated than traditional cellular networks. Thus, the interference coordination in OFDMA femtocell networks cannot be well handled by the existing schemes designed for macrocell deployments. There exist two kinds of interferences in OFDMA femtocell networks: interference between the macrocell and femtocell and the femtocell-to-femtocell interference. Orthogonalisation of resources in the frequency domain and/or in the time domain for the macrocell and femtocell can avoid the interference between the macrocell and femtocell, although it is inefficient in terms of spectrum reuse [10]. In [11], a frequency assignment scheme was proposed for femtocell networks while considering the handoff and interference between the macrocell and femtocell. However, since the number and position of BSs in femtocell networks are semi-statically varying, the femtocell-to-femtocell co-channel interference has to be dealt with by specifically designed radio resource allocation scheme. To the best of our knowledge, the channel allocation problem for coordinating the interference between femtocells has not been explicitly addressed in prior literature so far. With the constraint of maximum transmission power and minimum user rate, the centralised channel assignment with exhaustive search was performed to maximise the network throughput [12]. The optimisation problem of distributed power allocation between femtocells was solved by finding the Nash equilibrium [13]. In LTE cellular networks, each femtocell can be assigned a carrier after interacting with its neighbours based on the specified utility functions [14].

In OFDMA femtocell networks, the whole bandwidth is divided into orthogonal subcarriers, which are then grouped into subchannels. In this paper, we first formulate the channel allocation in the multi-cell OFDMA femtocell networks as an optimisation problem. Our objective is to achieve the maximum system throughput while ensuring proportional rate fairness among femtocells. However, there is no polynomial-time algorithm to obtain the optimal solution of this function. Therefore we propose a graph-based interference coordination scheme in order to avoid such prohibitive computation complexity.

The problem of allocating subchannels in a cellular network can be modelled as a graph theoretical colouring problem [15–17]. Different from the classic colouring problem that finds the minimum number of necessary colours, the channel allocation problem in femtocell networks is to determine how to assign a given number of colours (i.e. subchannels) to all the femtocells in order to achieve the specified objective. Since the on/off behaviours and locations of BSs in femtocell networks are semi-statically varying, our proposed scheme first constructs an interference graph for femtocells with the knowledge of the received signal-to-interference-plus-noise-ratio (SINR) derived from the received power of cell-specific reference signals. Then, all the femtocells are divided into the least number of groups, under the condition that there are no femtocells that interfere each other in the same group. Moreover, we maximise the sum throughput of each group during the division process. The femtocells in the same group can thus share the same subchannels while those in different groups must use orthogonal subchannels. In this way, the maximum frequency reuse factor can be achieved under the interference constraint. Finally, the original channel allocation problem is turned into the assignment of the given number of colours (i.e. subchannels) to each group in order to achieve the maximum system throughput while ensuring proportional fairness constraint, which in turn further reduces to determining the number of subchannels assigned to each group. We formulate this as a convex optimisation problem and its integer solution can be found by the approximation method.

The remainder of this paper is organised as follows. Section 2 gives a brief description of the system model and formulates the proportional fair (PF) channel allocation problem in OFDMA femtocell networks. A graph-based interference coordination scheme for OFDMA femtocell networks is proposed in Section 3. In Section 4, simulation results are presented. Finally, Section 5 concludes this paper.

2 System model and problem formulation

As shown in Fig. 1, a downlink network with N active femtocells is considered in this paper. Assume that M data subchannels are available for resource allocation. Usually, there are few users with very low or even no mobility in the home or office environment. We consider only one mobile station (MS) is connected to the BS per cell for simplicity [18]. Since the behaviours of BSs in femtocell networks are controlled by customers, the network topology of femtocell systems varies semi-statically, resulting in complex femtocell-to-femtocell co-channel interferences. The interferences among femtocells have to be coordinated through the well-designed channel allocation in order to achieve a good balance between an aggressive reuse of the spectral resource and the resulting co-channel interferences.

Let the binary matrix $\boldsymbol{A} = \{a_{m,n} | a_{m,n} \in \{0, 1\}\}_{M \times N}$ represent the channel allocation between femtocells, where

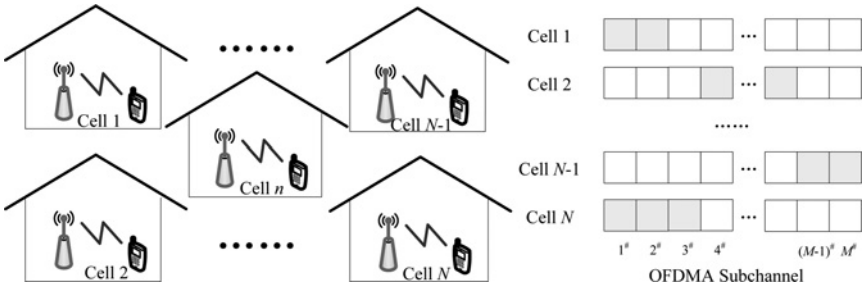

Fig. 1 *Illustration of OFDMA femtocell networks*

doi: 10.1049/iet-com.2011.0134

$a_{m,n} = 1$ denotes that subchannel m is assigned to femtocell n, and $a_{m,n} = 0$ otherwise. The achievable rate on subchannel m in femtocell n is given by

$$\eta_{m,n} = W \log_2\left(1 + \frac{L_{n,n}P_{m,n}}{\sum_{j=1,j\neq n}^{N} L_{n,j}a_{m,j}P_{m,j} + \sigma_N^2}\right), \quad 1 \le m \le M, \quad 1 \le n \le N \tag{1}$$

where W is the subchannel bandwidth, $P_{m,n}$ is the transmit power from the BS of femtocell n on subchannel m, $L_{n,j}$ is the path loss attenuation factor from BS j to the MS in femtocell n, and σ_N^2 is the noise power of the additive white Gaussian noise. For simplicity, the transmit power is the same for all BSs, that is, $P_{m,n} = P_T$, $1 \le m \le M$, $1 \le n \le N$.

The channel allocation problem is to find a mapping $\boldsymbol{A}$ between femtocells and subchannels. To achieve the maximum system throughput while ensuring the proportional rate fairness among femtocells, the sum of the logarithmic average cell throughput should be maximised [19]. Then, this problem can be formulated as the following optimisation function

$$\max_{\boldsymbol{A}} \sum_{n=1}^{N} \log\left(\sum_{m=1}^{M} a_{m,n} \cdot \eta_{m,n}\right) \tag{2}$$

Since (2) is non-concave to the binary variable $a_{m,n}$, this problem is NP-hard. There is no polynomial-time algorithm to obtain the optimal solution of $\boldsymbol{A}$. Therefore we propose a graph-based interference coordination scheme to decide how to allocate subchannels in OFDMA femtocell networks.

3 Proposed graph-based interference coordination scheme

Since the interference of subchannel m in femtocell n is dependent on the reuse of subchannel m in other femtocells, the SINR and the corresponding achievable rate $\eta_{m,n}$ are unknown until the channel allocation is decided. In other words, the interference and the channel allocation are dependent on each other. This makes the optimisation problem in (2) hard to be solved. Therefore we propose a graph-based interference coordination scheme to deal with the channel allocation problem in OFDMA femtocell networks, which turns the optimisation problem in (2) into a convex one by dividing the interfering femtocells into different groups based on the interference graph.

3.1 Construct the interference graph

Let us first formulate the inter-cell interference between femtocells by an interference graph. Based on a given network topology, the interference graph $\boldsymbol{G} = (\boldsymbol{V}, \boldsymbol{E})$ can be constructed. The vertex set $\boldsymbol{V}$ and edge set $\boldsymbol{E}$ denote femtocells and the potential interferences between femtocells, respectively.

As stated before, the exact value of the interference for femtocell n in subchannel m is not available until the channel allocation is performed. It is dependent on the allocation of subchannel m to other femtocells, which is unknown before the problem in (2) is solved. Then, the interference graph is constructed by measuring the received power of the cell-specific reference signal, which is transmitted by each femtocell BS with the cell-specified scrambling sequence [20]. On the assumption that one subchannel in femtocell n is reused by femtocell k, the received SINR of the user in femtocell n can be expressed by

$$\hat{\gamma}_{n,k} = \frac{L_{n,n}P_T}{L_{n,k}P_T + \sigma_N^2}, \quad 1 \le n,\ k \le N \tag{3}$$

An edge (v_n, v_k) exists if and only if the received SINR in either femtocell n or femtocell k is below the required communication threshold Γ_{th} if the subchannel is reused by them, that is

$$\min\{\hat{\gamma}_{n,k}, \hat{\gamma}_{k,n}\} \le \Gamma_{\text{th}} \tag{4}$$

The same subchannel cannot be reused by two femtocells if the edge exists.

Next, by mapping each subchannel onto a colour, we have the colour set $\boldsymbol{F}$, whose size equals to the number of subchannels, that is, M. So, the channel allocation problem is equivalent to how to colour each vertex in set $\boldsymbol{V}$ with a number of colours in set $\boldsymbol{F}$. The traditional channel allocation problem aims at minimising the required number of subchannels (i.e. colours) under the interference constraint. In OFDMA femtocell networks, it becomes to obtain the channel allocation with the fixed number of subchannels while maximising the sum of logarithmic cell rate on the condition of the acceptable interference as specified in (4).

3.2 Partitioning of femtocells into groups

With the knowledge of the interference graph, we partition all the femtocells into different groups, where subchannels are fully reused or orthogonally allocated between femtocells in the same or different groups, respectively. Considering the close relationship between the colouring problem in the graph theory and the interference coordination problem in OFDMA networks, we apply the greedy graph colouring algorithm to decide how to divide the femtocells into groups under the acceptable inter-cell interference as specified in (4). In each stage of the partition procedure, the group which has the maximum sum throughput is selected in order to exploit the potential overall system capacity as much as possible.

The colouring of a graph $\boldsymbol{G} = (\boldsymbol{V}, \boldsymbol{E})$ is to assign the colours to the vertex set $\boldsymbol{V}$ while no two vertices with an edge have the same colour. The smallest number of colours needed to colour a graph $\boldsymbol{G}$ is called its chromatic number, that is, K. A subset of vertices assigned to the same colour is called a colour class, which forms an independent set. Thus, the greedy colouring is the same as a partition of the vertex set into K independent sets. The femtocells in the same independent set will be assigned with the same subchannels, that is, colours. The fewer the number of colours used in an interference graph $\boldsymbol{G}$, the higher the frequency reuse factor that can be achieved in OFDMA femtocell networks.

By using the greedy graph colouring, all the vertices are partitioned into K independent groups through K stages successively. In the kth stage ($0 \le k \le K$), a heuristic algorithm, called as simulated annealing (SA), is used for searching the maximum independent sets (MISs), whose details can be found in Appendix 1 [21]. It has a high probability of finding the optimal or a near-optimal solution in a reasonable amount of time by using simulated

annealing. After finding $Q_k \geq 1$ possible MISs, that is, $\{\tilde{\boldsymbol{V}}_k^{(1)}, \tilde{\boldsymbol{V}}_k^{(2)}, \ldots, \tilde{\boldsymbol{V}}_k^{(Q_k)}\}$, we have to determine how to select one of them as the kth group of femtocells. There is no SINR difference on the subchannels assigned to femtocell n because all of them are reused by the femtocells in the same groups. So, the subchannel index m can be omitted in the following description. Then, on the assumption that the qth MIS is selected in the kth stage, the achievable rate per subchannel at femtocell n in $\boldsymbol{V}_k^{(q)}$ can be expressed by

$$\tilde{\eta}_n^{(q)} = W \log_2\left(1 + \frac{L_{n,n}P_T}{\sum_{v_j \in \boldsymbol{V}_k^{(q)}, j \neq n} L_{n,j}P_T + \sigma_N^2}\right), \quad v_n \in \tilde{\boldsymbol{V}}_k^{(q)} \tag{5}$$

Different MISs include different femtocells and each femtocell has a different location, resulting in different achievable rates. In order to achieve the maximum system throughput, the MIS with the maximum sum of the cell rates is chosen in each stage, that is

$$\tilde{\boldsymbol{V}}_k = \arg\max_{\tilde{\boldsymbol{V}}_k^{(q)}} \sum_{v_n \in \tilde{\boldsymbol{V}}_k^{(q)}} \tilde{\eta}_n^{(q)}, \quad 1 \leq q \leq Q_k \tag{6}$$

All the vertices in the selected MIS are assigned with one or more than one available colours (i.e. subchannels) and deleted from the graph. Then, the remaining vertices in the graph are used to establish a graph colouring subproblem in the next stage. This process repeats until no smaller MIS can be found.

3.3 Channel allocation between the groups

After the partition, all the femtocells are divided into K groups with the acceptable interference condition. The subchannels are orthogonally allocated between femtocells in different groups. Next, we need to determine how to allocate all the subchannels into different groups. Assuming that subchannels are fully reused between femtocells in the same group, the received SINRs of subchannels of a user in the certain location have no difference since only the path loss of links is considered in this paper. So, the original channel allocation problem in (2) is reduced as the problem how many subchannels should be assigned to each group, that is

$$\begin{aligned} &\max_B \sum_{n=1}^{N} \log\left(\sum_{k=1}^{K} b_{n,k} s_k \cdot \tilde{\eta}_n\right) \\ &\text{subject to} \sum_{k=1}^{K} s_k = M, \\ &\sum_{k=1}^{K} b_{n,k} = 1 \end{aligned} \tag{7}$$

where $\tilde{\eta}_n$ is the transmission rate of BS in the nth femtocell on the allocated subchannels, s_k is the number of subchannels assigned to the kth group, $b_{n,k} = 1$ means that the nth femtocell is grouped into the kth group, and $b_{n,k} = 0$ otherwise, that is

$$b_{n,k} = \begin{cases} 1, & v_n \in \tilde{\boldsymbol{V}}_k \\ 0, & \text{otherwise} \end{cases} \tag{8}$$

Let $S = \{s_k | s_k \in \{0, 1, 2, \ldots, M\}\}_{1\times K}$ describe the channel allocation between the sets. As proved by Appendix 2, this optimisation problem in (7) is equivalent to

$$\begin{aligned} &\max_{\mathbf{s}} \sum_{k=1}^{K} g_k \log s_k \\ &\text{subject to} \sum_{k=1}^{K} s_k = M \end{aligned} \tag{9}$$

where g_k is the number of femtocells in the kth group.

This problem is strictly convex when s_k is a real number. Then, the Lagrangian function associated with problem in (9) can be written as

$$L(s_k, \lambda) = \sum_{k=1}^{K} g_k \log s_k - \lambda\left(\sum_{k=1}^{K} s_k - M\right) \tag{10}$$

where $\lambda \geq 0$ is the Lagrangian variable which makes $\sum_{k=1}^{K} s_k = M$.

Taking the derivative of (10) on s_k and let its value equals zero, the optimal real-value s_k can be easily calculated by

$$s_k^{\text{real}} = g_k M / N \tag{11}$$

However, the optimal solution in (11) may produce fractional subchannel allocation. In other words, the number of subchannels allocated to each group should be integer while s_k^{real} may not. Therefore we propose an approximation method to find the integral solution, which is described in Fig. 2. s_k is initialised to the round value of s_k^{real}. If the sum of all the s_k is equal to M, no further operation is needed. Otherwise, s_k is assigned to $\lfloor S_k^{\text{real}} \rfloor$. Then, there are $S_L = M - \sum_{i=1}^{k} s_i$ subchannels left, which are further allocated one by one to S_L sets with larger decimal part of s_k^{real}. The s_k of the sets with one more subchannel is increased to $\lfloor S_k^{\text{real}} \rfloor + 1$ while others are unchanged.

4 Simulation results

In this section, simulation results are presented to evaluate the performance of the proposed channel allocation method in OFDMA femtocell networks, where the dense femtocell deployment scenario is assumed and modelled [18, 22]. For simplicity, only one femtocell block is considered. As shown in Fig. 3, each femtocell block consists of two stripes of apartments, and each stripe has 2 by N_D apartments (e.g. N_D is set to 10 as illustrated in Fig. 3). Each apartment with the size of 10 m × 10 m may have a femtocell. There is a street with width of 10 m between two stripes of apartments. Each femtocell block has L_D floors, which can be chosen randomly between 1 and 10 (e.g. $L_D = 6$ $L_D = 6$ in our simulations).

To simulate the realistic case where an apartment may not have a femtocell, a parameter of deployment ratio ρ is used to determine whether an apartment is deployed with a femtocell or not. Since femtocells are not always on, we defined another parameter of activation ratio β to describe the percentage of active femtocells. Only when a femtocell is active, it transmits with the given power at traffic subchannels. Otherwise, it keeps silent at traffic subchannels. The activation ratio β can be varied from 0 to 100%. Both the femtocell BS and the MS are distributed uniformly at

doi: 10.1049/iet-com.2011.0134

Input: $\mathbf{G} = \{g_k | g_k \in \{0, 1, 2, \cdots, N\}, 1 \leq k \leq K\}$ is a vector indicating the number of femtocells in all the K sets.
Output: $\mathbf{S} = \{s_k | s_k \in \{0, 1, 2, \cdots, M\}, 1 \leq k \leq K\}$ is a vector of the number of subchannels allocated to each cluster.
Initialisation: $s_k = round(s_k^{real})$.
if $sum\,(s_k) == M$ **then**
  return $\mathbf{S} = \{s_k | s_k \in \{0, 1, 2, \cdots, M\}, 1 \leq k \leq K\}$.
else
  $s_k = \lfloor s_k^{real} \rfloor$.
  $S_L = M - \sum_{i=1}^{k} s_i$.
  Sort the sets by the decimal part of s_k^{real} in a descending order.
  S_L subchannels are allocated one by one to the first S_L sets of the re-ordered sets.
  Update the corresponding $s_k = \lfloor s_k^{real} \rfloor + 1$.
  return $\mathbf{S} = \{s_k | s_k \in \{0, 1, 2, \cdots, M\}, 1 \leq k \leq K\}$.
end if

Fig. 2 *Approximation method to find the suboptimal solution of s_k*

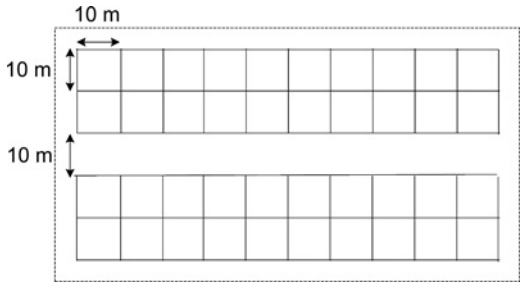

Fig. 3 *Illustration of a femtocell block*

random in the apartment. Most of simulation parameters closely follow the 3G LTE-A network as summarised in Table 1 [4]. The number of available subchannels is 50 with a 10 MHz bandwidth, that is, $M = 50$. When $\rho = 0.2$ and $\beta = 50\%$, it means that on average each floor has four active femtocells and each block has active 24 femtocells under the given configuration, that is, $N = 24$. If the deployment ratio ρ is increased to 0.4 with $\beta = 50\%$, there are more average active femtocells in one block, that is, $N = 48$.

4.1 Effects of the required communication threshold

As described in (4), the construction of interference graph is based on the comparison results between the received SINR and the required communication threshold Γ_{th}. Fig. 4 shows an example of the interference graph generated in simulations. Given the scenario of $\rho = 0.2$ or 0.4 and $\beta = 50\%$, different interference graphs will be generated with different values of the threshold. In Fig. 5, we compare the cumulative distribution function (CDF) of the received SINR in the network with different thresholds in the proposed channel allocation schemes. When the value of the threshold decreases, less number of edges exists in the interference graph. Then, the MISs of the interference graph may include more vertices. In other words, more femtocells are grouped into the same cluster and can reuse the same subchannels. In this way, higher frequency reuse factor can be achieved while more serious co-channel interference is caused. Therefore the SINR performances become worse when the threshold becomes smaller.

The performance of the proposed scheme is evaluated in terms of efficiency and fairness. The efficiency can be demonstrated by the average throughput while the fairness is by the cell edge throughput. Usually, the cell edge throughput is defined as the 5% point of the CDF of the user throughput [23]. As shown in Fig. 6, the average throughput (TP) performance of the network with our

Table 1 Simulation parameters in OFDMA femtocell networks

Parameters	Values
carrier bandwidth	10 MHz
number of subchannel	50
min separation UE to femto BS	1 m
number transmit antennas femto BS	1
number receive antennas UE	2
femto BS antenna gain	5 dBi
path loss model femto BS to UE (dB)	$127 + 30\log10(R/1000)$, R in m
shadowing standard deviation	8 dB
noise figure UE	9 dB
transmit power femto BS	20 dBm
number of user per femtocell	1
traffic model	full buffer

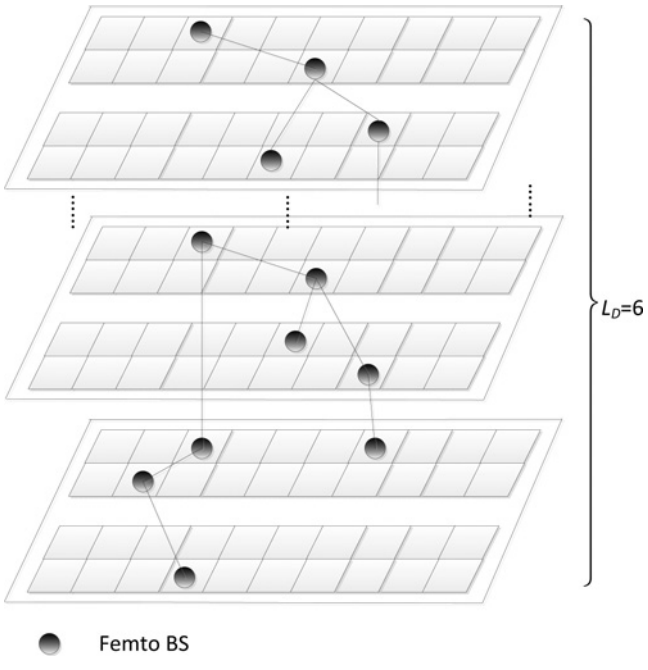

Fig. 4 *Example of interference graph*

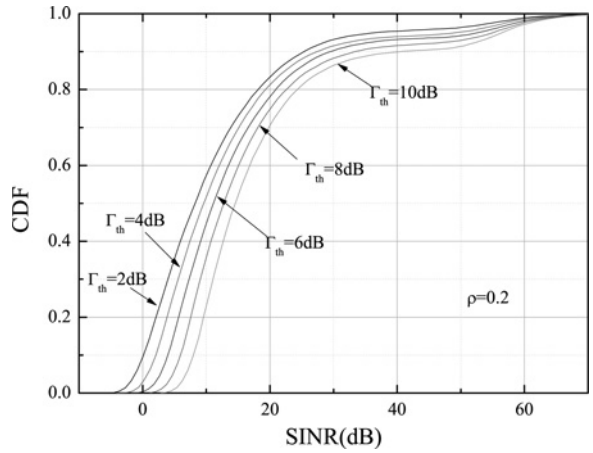

Fig. 5 *CDF of SINR with different required communication threshold*

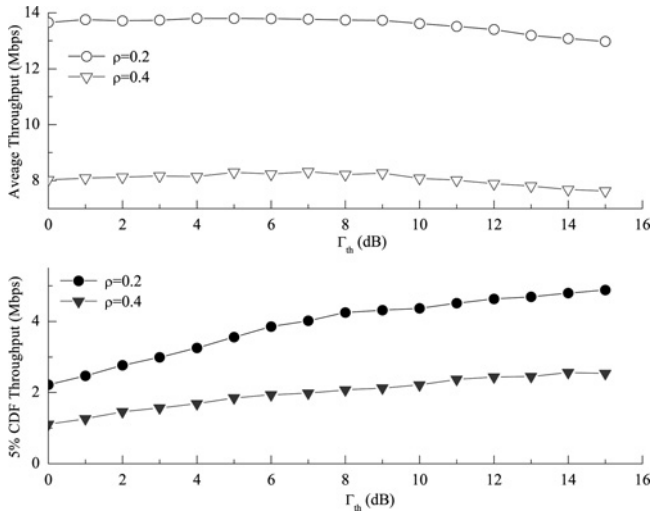

Fig. 6 *Throughput performances with different required communication threshold*

proposed channel allocation method is improved with the decrease of the threshold Γ_{th}, since subchannels are reused by femtocells more frequently. Note that the threshold Γ_{th} is not allowed to be too small since it is used to guarantee the acceptable packet error rate in practical applications. On the other hand, the throughput performances at the 5% CDF become worse when the threshold grows smaller. This is because the femtocells with low received SINRs are more sensitive to the interference than those having high received SINRs. Therefore their throughput is deteriorated with the smaller threshold value even though more subchannels are allocated. Considering the tradeoff between the average throughput (i.e. effectiveness) and the throughput at the 5% CDF (i.e. fairness), we set the threshold value to be 8 dB for the simulations under the scenario of $\rho = 0.2$ or 0.4 and $\beta = 50\%$. Note that the throughput at the 5% CDF decreases more rapidly when the threshold value becomes smaller than 8 dB.

4.2 Comparison between different channel allocation schemes

The performance of the network with the optimal channel allocation scheme is also presented for comparison, that is, the optimal solution in (2). This solution has the prohibitive computation complexity of $O(N^2M \cdot 2^{MN})$. So, we reduce the number of the femtocells and subchannels (i.e. N and M) in order to make the exhaustive search possible. Three simple scenarios are defined for the sake of comparison, that is, Case 1 ($N \times M = 3 \times 4$), Case 2 ($N \times M = 4 \times 4$) and Case 3 ($N \times M = 4 \times 5$). Fig. 7 presents the throughput CDF of the optimal and proposed schemes under different cases. It is shown that the proposed scheme can achieve almost the same throughput performance as the optimal one. To better show the performance difference, we also presented the average throughout and the throughput at the 5% CDF of the networks by the optimal and proposed schemes in Fig. 8. Compared with the optimal scheme, there is only slight performance reduction in terms of the average throughput and the throughput at the 5% CDF when the proposed scheme is applied in the network under different configurations, for example, 3.3 and 4.5% under Case 1, 4.8 and 3.2% under Case 2 and 4.2 and 5.9% under Case 3, respectively. Moreover, the proposed scheme has the acceptable computation complexity of $O(N^2 + N^2 \log N + N^2K + K)$.

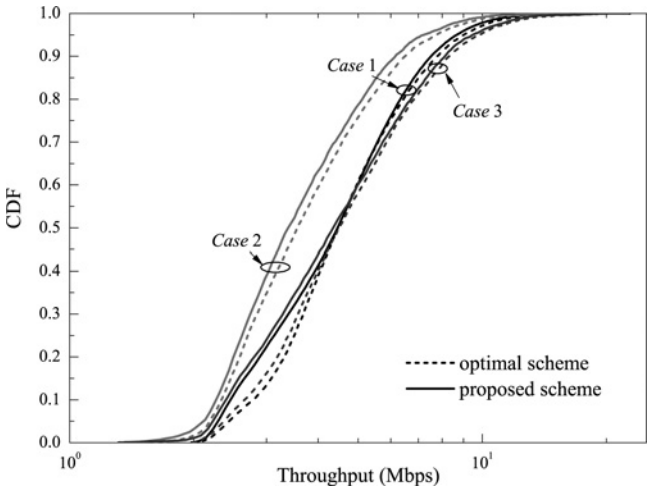

Fig. 7 *CDF of user throughput with the optimal and proposed schemes*

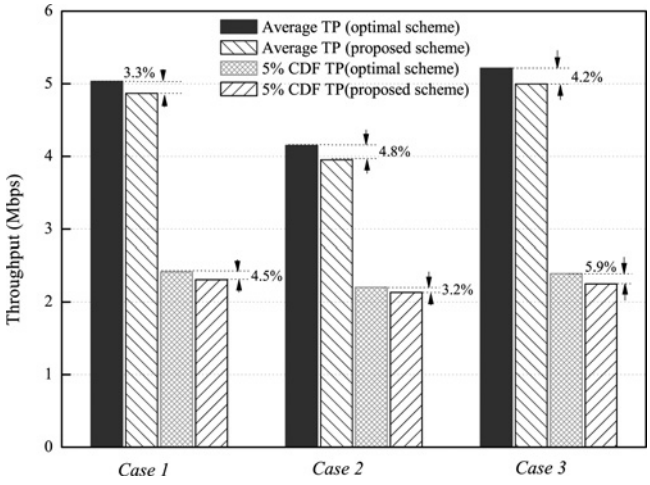

Fig. 8 *Throughput comparison between the optimal and proposed schemes*

doi: 10.1049/iet-com.2011.0134

There are several well-known fairness indexes used to measure the fairness in communication networks [24], for example, general proportional fairness (GPF) index, Gini index, Jain fairness index, min–max index, and so on. Since the PF objective is the focus of this paper, the GPF index is used as the fairness metric to evaluate the proposed scheme, which is defined as [25]

$$I_{\mathrm{GPF}} = \sum_{n=1}^{N} \log \eta_n \tag{12}$$

where η_n is the average transmission rate of the user in the nth femtocell. As shown in Fig. 9, we compare the GPF index performances of the optimal scheme and the proposed scheme under simple scenarios. From the viewpoint of maximising the sum of the logarithmic cell throughput, higher GPF index means better fairness performance. We observe that the proposed scheme has a smaller GPF than the optimal scheme. However, the difference between them is quite small, which means that our proposed scheme can achieve almost the same fairness performance as the optimal one.

Next, we compare the performance of the different channel allocation schemes under the complex scenario, that is, $L_D = 6$ and $M = 50$. With the orthogonal channel allocation scheme (i.e. Scheme 1), the subchannels are assigned to each femtocell by the round robin (RR) principle. Moreover, in order to clearly verify the effectiveness of different steps in the proposed scheme, we define another channel allocation scheme (i.e. Scheme 2) as a reference, that is, the subchannels are evenly allocated to groups, which are partitioned by the greedy colouring algorithm. Figs. 10 and 11 show the CDF of throughput with the different channel allocation schemes, where the deployment ratio ρ is set to 0.2 and 0.4, respectively. It can be seen that the proposed channel allocation scheme has a remarkable improvement in the throughput performance compared to the other two schemes. We also see that both steps in the proposed scheme have significant effects on the performance gain. In addition, due to the fixed number of subchannels and higher interference with the increase of deployment ratio, a smaller per cent of femtocells can achieve high throughput. For example, with the proposed scheme, about 57% of femtocells have the throughput larger than 10 Mbps for $\rho = 0.2$ and only 27% of femtocells for $\rho = 0.4$.

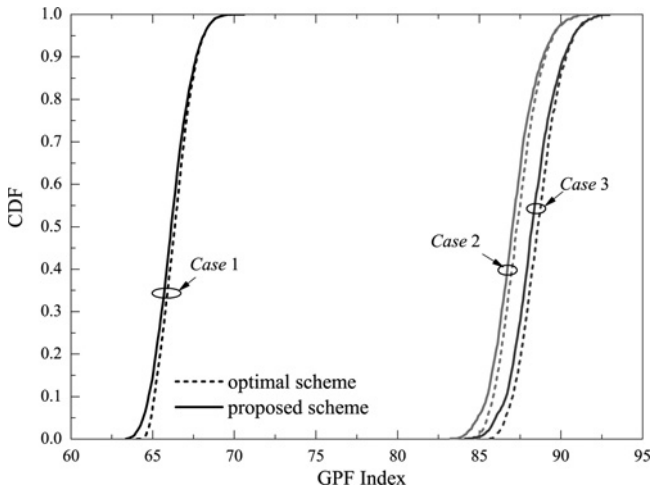

Fig. 9 *CDF of GPF index with the optimal and proposed schemes*

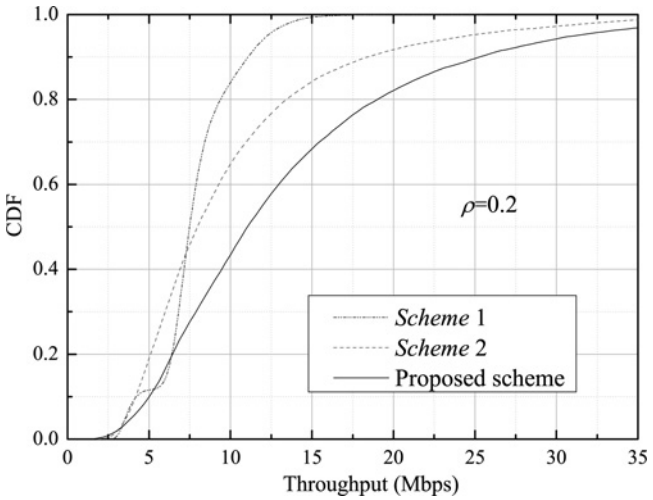

Fig. 10 *CDF of user throughput with different resource partition schemes with $\rho = 0.2$*

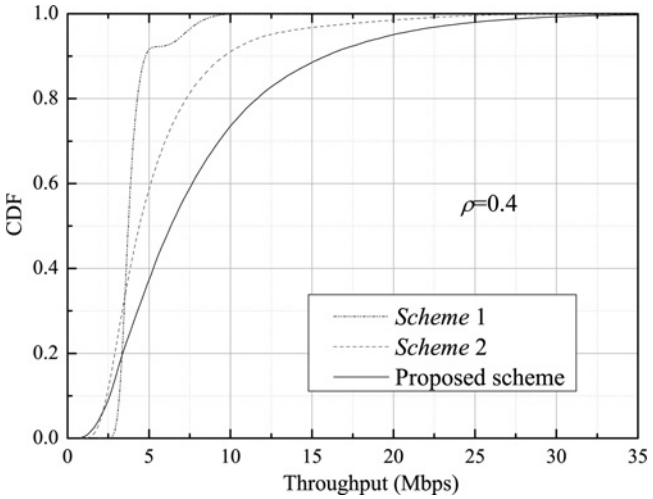

Fig. 11 *CDF of user throughput with different resource partition schemes with $\rho = 0.4$*

Table 2 Throughput comparison between different channel allocation schemes

	$\rho = 0.2$		$\rho = 0.4$	
	Average TP, Mbps	Total TP, Mbps	Average TP, Mbps	Total TP, Mbps
Scheme 1	7.8722	188.93	4.0721	195.46
Scheme 2	10.315	247.56	5.6601	271.68
proposed scheme	13.686	328.46	8.2185	394.49

Correspondingly, the average cell throughput and the total throughput of all cells in the networks with different channel allocation schemes are compared in Table 2. We can observe significant gains on not only the average throughput but also the total throughput by using the proposed scheme. Since the subchannels are allocated orthogonally with a given number

of subchannels by Scheme 1, the total throughput does not change with the increase of deployment ratio. On the other hand, the number of active femtocells increases with the deployment ratio ρ, which means fewer number of subchannels may be assigned to one group and higher interference exists in each group of the network with the proposed scheme. So, the corresponding average cell throughput decreases with the increase of the deployment ratio. However, the total throughput of the networks with the proposed scheme still increases with a higher deployment ratio because more active femtocells may reuse the subchannels more frequently.

5 Conclusion

In this paper, we presented a framework of channel allocation in OFDMA femtocell network with a graphical approach. Our proposed graph-based technique explicitly uses the SINR to generate the interference graph from OFDMA femtocell networks to guarantee the acceptable inter-cell interference for all links. The femtocells are partitioned into different groups by the greedy graph colouring algorithm, where the reused and orthogonal subchannels are assigned to the femtocells in the same and different groups, respectively. Since the number of groups is minimised by graphic colouring, the spectrum efficiency is improved. Then, to maximise the sum of logarithmic cell rates with the acceptable inter-cell interference, the number of subchannels allocated to each group linearly increases with the size of the group. Our simulation results show that the required communication threshold for constructing the interference graph has to be properly selected in order to achieve good tradeoff between effectiveness and fairness. Also, compared with optimal channel allocation scheme, the proposed scheme can reduce the computational complexity at the cost of a slight degradation of throughput and fairness performance. Moreover, it can achieve significant performance improvement over other orthogonal channel allocation schemes in terms of the average cell throughput and the total throughput.

6 Acknowledgments

This work was supported in part by National Basic Research Program of China (973 Program) under grant 2012CB316005, National Key Technology R&D Program of China under grant 2009ZX03003-008-01 and Research Fund for the Doctoral Program of Higher Education under grant 200800131023.

7 References

1 Knisely, D.N., Yoshizawa, T., Favichia, F.: 'Standardization of femtocells in 3GPP', *IEEE Commun. Mag.*, 2009, **47**, (9), pp. 68–75
2 Knisely, D.N., Favichia, F.: 'Standardization of femtocells in 3GPP2', *IEEE Commun. Mag.*, 2009, **47**, (9), pp. 76–82
3 Kim, R.Y., Kwak, J.S., Etemad, K.: 'WiMAX femtocell: requirements, challenges, and solutions', *IEEE Commun. Mag.*, 2009, **47**, (9), pp. 84–91
4 3GPP TR 36.814, v1.2.1.: 'Further advancements for E-UTRA, physical layer aspects', August 2009
5 Chandrasekhar, V., Andrews, J., Gatherer, A.: 'Femtocell networks: a survey', *IEEE Commun. Mag.*, 2008, **46**, (9), pp. 59–67
6 3GPP R1-060864.: 'Overview of resource management techniques for interference mitigation in EUTRA'. Texas Instruments, 3GPP TSG RAN WG1 Meeting #44bis, March 2006
7 3GPP R1-050507.: 'Soft frequency reuse scheme for UTRAN LTE'. Huawei, 3GPP TSG RAN WG1 Meeting #41, May 2005
8 3GPP R1-060689.: 'System simulation results for downlink interference coordination'. Alcatel, 3GPP TSG RAN WG1 Meeting #44, February 2006
9 Saad, G.K., David, G.: 'Optimal and distributed scheduling for multicell capacity maximization', *IEEE Trans. Wirel. Commun.*, 2008, **7**, (1), pp. 288–298
10 Chandrasekhar, V., Andrews, J.G.: 'Spectrum allocation in two-tier networks'. Asilomar Conf. Signals, Systems and Computers, October 2008, pp. 1583–1587
11 Guvenc, I., Moo-Ryong, J., Watanabe, F., Inamura, H.: 'A hybrid frequency assignment for femtocells and coverage area analysis for co-channel operation', *IEEE Commun. Lett.*, 2008, **12**, (12), pp. 880–882
12 Ling, J., Chizhik, D., Valenzuela, R.: 'On resource allocation in dense femto-deployments'. IEEE Int. Conf. Microwaves, Communications, Antennas and Electronics Systems, November 2009, pp. 1–6
13 Hong, W., Tsai, Z.: 'On the femtocell-based MVNO model: a game theoretic approach for optimal power setting'. IEEE Vehicular Technology Conference (VTC 2010-Spring), May 2010, pp. 1–5
14 Zheng, K., Hu, F., Lei, L., Wang, W.: 'Interference coordination between femtocells in LTE-advanced networks with carrier aggregation'. IEEE Int. Conf. Communications and Networking in China, August 2010, pp. 1–5
15 Youngs, D.: 'Frequency assignment for cellular radio networks'. IEE Conf. Telecommunications, 1995, pp. 179–183
16 Chang, Y.-J., Tao, Z., Zhang, J., Kuo, C.-C.J.: 'A graph-based approach to multi-cell OFDMA downlink resource allocation'. IEEE Global Telecommunications Conf., 2008, pp. 1–6
17 Brzezinski, A., Zussman, G., Modiano, E.: 'Distributed throughput maximization in wireless mesh networks via pre-partitioning', *IEEE/ACM Trans. Netw.*, 2008, **16**, (6), pp. 1406–1419
18 Femto Forum Working Group 2 Document: 'OFDMA interference study: evaluation methodology document', March 2009
19 Boudec, J.-Y.: 'Rate adaptation, congestion control and fairness: a tutorial', http://www.epfl.ch/PS_files/LEB3132.pdf
20 3GPP TS 36.211 V8.8.0: 'Evolved universal terrestrial radio access (E-UTRA): physical channels and modulation', September 2009
21 Johnson, E.M.: 'Simulated annealing and optimization', *Am. J. Math. Manage. Sci.*, 1988, **8**, (3–4), pp. 205–450
22 3GPP R4-092042: 'Simulation assumptions and parameters for FDD HeNB RF requirements'. May 2009
23 3GPP TR 25.814 V7.1.0: 'Physical layer aspects for evolved universal terrestrial radio access (UTRA) (Release 7)', September 2006
24 Dianati, M., Shen, X., Naik, S.: 'A new fairness index for radio resource allocation in wireless networks'. IEEE Wireless Communications and Networking Conf., 2005, Vol. 2, pp. 712–717
25 Kaneko, M., Popovski, P., Dahl, J.: 'Proportional fairness in multi-carrier system: upper bound and approximation algorithms', *IEEE Commun. Lett.*, 2006, **10**, (6), pp. 462–464

8 Appendix 1

8.1 Details of simulated-annealing algorithm

After initialisation, the iterations, called as metropolis procedure are carried out. In the ith iteration, a cost function C_i is first computed, which depends not only on the current independent set (CIS) $\boldsymbol{C}_i$ but also on the edges $\boldsymbol{E}_i$ existing in this CIS. The search for MIS proceeds with the cost function, reducing most of the time. In each iteration, the CIS will be generated by dealing with the vertex, which is randomly selected from $\boldsymbol{V}$. Then, we calculate the cost difference $\Delta C = C_i - C_{i-1}$ by updating the CIS. The criterion for accepting or rejecting the update of CIS depends upon computing not only the cost difference $\Delta C = C_i - C_{i-1}$ but also the ratio between the probability of the system being in $\boldsymbol{C}_i$ and the probability of being in $\boldsymbol{C}_{i-1}$, that is, $\zeta = e^{-\Delta C/t}$. Before the metropolis procedure is repeated, the temperature is decreased according to an appropriate annealing rule. The annealing process is terminated when there is no update of CIS accepted, that is, no vertex is added into or removed from the CIS. See Fig. 12 for details.

Input: $\mathbf{G} = (\mathbf{V}, \mathbf{E})$ is the the interference graph.
Output: $\tilde{\mathbf{V}}$ is a MIS of graph $\mathbf{G}$.
Initialisation: Initialise the values of the temperature t, the attenuation factor dt, the iterative times, the control state S and the CIS $\mathbf{C}_i$, i.e. $t = 1$, $dt = 0.9$, $N_I = 500$, $S = 0$ and $\mathbf{C}_i = \varnothing, i \in \{0, 1, \cdots, N_I\}$.
while TRUE **do**
  $flag = 0$.
  for $i = 1 : N_I$ **do**
    $C_i = f(\mathbf{C}_i, \mathbf{E}_i)$.
    Select a vertex $v \in \mathbf{V}$ randomly.
    if $v \notin \mathbf{C}_{i-1}$ **then**,
      $\mathbf{C}_i = \{v\} \bigcup \mathbf{C}_{i-1}$.
    else
      $\mathbf{C}_i = \mathbf{C}_{i-1} - \{v\}$.
    end if
    Calculate the difference of cost function $\triangle C = C_i - C_{i-1}$.
    if $\triangle C < 0$ or $e^{-\triangle C/t} > \varepsilon, \varepsilon \sim U(0, 1)$ **then**
      $\tilde{\mathbf{V}} = \mathbf{C}_i$.
      $flag = 1$.
    else
      $\tilde{\mathbf{V}} = \mathbf{C}_{i-1}$.
    end if
  end for
  Decrease the temperature $t = t * dt$.
  if $flag == 0$ **then**
    $S = S + 1$.
  else
    $S = 0$.
  end if
  if $S == 2$ **then**
    Break.
    return $\tilde{\mathbf{V}}$.
  end if
end while

Fig. 12 *Simulated-annealing algorithm to search MIS*

9 Appendix 2

9.1 Proof of the equivalence from (7) to (9)

As in (6), when the MIS is selected, $\tilde{\eta}_n$ can be computed, that is

$$\tilde{\eta}_n = W \log_2\left(1 + \frac{L_{n,n}P_T}{\sum_{v_j \in \tilde{V}_k, j \neq n} L_{n,j}P_T + \sigma_N^2}\right), \quad v_n \in \tilde{V}_k \tag{13}$$

So, the part of $\sum_{n=1}^{N} \log \tilde{\eta}_n$ in (7) can be regarded as a constant and omitted. Then, the maximisation in (7) can be equivalently rewritten as

$$\begin{aligned}\max_{\boldsymbol{B}} \sum_{n=1}^{N} \log\left(\sum_{k=1}^{K} b_{n,k}s_k \cdot \tilde{\eta}_n\right) &= \max_{\boldsymbol{B}} \sum_{n=1}^{N} \log\left(\sum_{k=1}^{K} b_{n,k}s_k\right) + \sum_{n=1}^{N} \log \tilde{\eta}_n \\ &= \max_{\boldsymbol{B}} \sum_{n=1}^{N} \log\left(\sum_{k=1}^{K} b_{n,k}s_k\right)\end{aligned} \tag{14}$$

Further derivation is carried on as follows:

$$\begin{aligned}&\sum_{n=1}^{N} \log\left(\sum_{k=1}^{K} b_{n,k}s_k\right) \\ &= \sum_{n=1, n\in\tilde{V}_1}^{N} \log\left(\sum_{k=1}^{K} b_{n,k}s_k\right) + \sum_{n=1, n\in\tilde{V}_2}^{N} \log\left(\sum_{k=1}^{K} b_{n,k}s_k\right) + \cdots \\ &\quad + \sum_{n=1, n\in\tilde{V}_K}^{N} \log\left(\sum_{k=1}^{K} b_{n,k}s_k\right) \\ &= \sum_{n=1, n\in\tilde{V}_1}^{N} \log s_1 + \sum_{n=1, n\in\tilde{V}_2}^{N} \log s_2 + \cdots \sum_{n=1, n\in\tilde{V}_K}^{N} \log s_K \\ &= \sum_{k=1}^{K} g_k \log s_k\end{aligned} \tag{15}$$

where $g_k = \sum_{n=1}^{N} b_{n,k}$ is the number of femtocells in the kth group. Therefore the optimisation problem in (7) can be equivalent to (9).